SOBENA

23º Congresso Nacional de Transporte Aquaviário, Construção Naval e Offshore

Rio de Janeiro, 25 a 29 de Outubro de 2010

THERMO-MECHANICAL ANALYSES OF HP/HT PIPELINES WITH SLIDING FOUNDATION END STRUCTURES

Daniel Carneiro*
Adriano Castelo
Bureau Veritas

Abstract:

Non-buried subsea pipelines subjected to high internal pressures and high operational temperatures (HP/HT) might experience significant axial expansion. If this movement is restrained by an end structure, considerable loads can be imposed to the system. Sliding foundations have been used to minimize this effect, allowing free end displacement despite the equipment.

However, thermo-mechanical behavior of HP/HT pipelines interacts with the end restrains in a complex manner. Axial displacements can accumulate over the operational cycles, in the phenomenon known as “pipeline walking”. If the sliding foundation design does not account for these accumulated displacements, axial loads (not considered in the pipeline design) might be imposed. As a result, the overall thermo-mechanical behavior in terms of lateral buckling and walking can change significantly.

This paper presents the results of finite element analyses performed to verify the importance of this interaction between the thermo-mechanical loads and the non-linear end restrain. The analyses were performed using highly non-linear tri-dimensional finite element models considering pipe-soil interaction with full 3D seabed bathymetry and load history maintained from pipe lay to operational cycles. The limited sliding range was imposed to the model ends. The results show that the pipeline global behavior after a few operational cycles is significantly different from the foreseen for the initial condition.

1 – Introduction

Flowlines are used to convey fluids used and/or produced in offshore oil and gas production systems. For relatively longer distances, the use of rigid steel pipelines might be economically advantageous if compared to flexible pipe. Despite the simple cross section, rigid flowlines are subjected to different concerns from the installation process up to the operational condition. Some particular issues associated to high pressure and high temperature (HP/HT) content are discussed in this paper.

When subjected to increments of temperature and internal pressure, a pipeline tends to expand axially. The soil friction resists to this elongation inducing axial compression to the pipeline, which might buckle globally as a column. During an operation shutdown, the temperature and pressure might be reduced so the pipeline will tend to contract back. Asymmetries in this expansion and contraction mechanism might accumulate large global axial movements along the design life, in a ratcheting process called by many authors “pipeline walking”.

Attachments to the pipeline such as end equipments interfere in the soil friction distribution as they imply in large weights and contact areas within short sections of pipe. Sliding foundations has been designed for pipeline end terminations (PLETs), which are skids (usually installed together with the pipeline) containing (ROV operated) valves and templates for connecting a jumper (either flexible or rigid). An example of PLET with sliding foundation is shown in Figure 1. When the pipeline is susceptible to axial ratcheting, the design of sliding mechanisms for the end structures is not trivial, as shown hereafter.

* Corresponding author:
daniel.carneiro@br.bureauveritas.com

This paper presents a review of the basic concepts of global thermo-mechanical behavior of pipelines, followed by some results of finite element analyses of recently installed flowlines. The PLETs with sliding foundations were considered in the analyses, thus the results illustrate the additional issues to be accounted for in the design of such mechanism.

2 – Nomenclature

α	Coefficient of axial thermal expansion;
Δp_i	Increment of internal pressure;
ΔT	Temperature increment;
ε	Mechanical strain;
ν	Poisson coefficient;
A_s	Pipe steel wall cross section area;
A_i	Pipe internal cross section area;
E	Young's modulus;
f	Soil axial resistance per unit length;
FE	Finite element;
HP/HT	High pressure and high temperature;
KP	Kilometer post;
L	Pipeline length;
P	Axial compressive force;
PLET	Pipeline end termination;
R	Soil axial resistance at the PLETs;
ROV	Remote operated vehicle.

3 – Thermo-mechanical behavior

If a temperature increment ΔT is applied to a section of pipeline of length L which is totally free to expand, it will grow up to a new length $(1 + \alpha\ \Delta T)L$. If otherwise the pipeline is fully restrained and will maintain its original length L, the restraining will impose an axial compression to the pipe wall. The level of this compression is so to induce an axial mechanic strain $\varepsilon = -\alpha\ \Delta T$ (where the negative signal indicate that this strain is compressive for positive ΔT) that will nullify the thermal expansion. The magnitude of the resulting compression for the totally restrained pipeline is $P = E\ A_s\ \alpha\ \Delta T$. There is obviously the intermediate condition (e.g. when the compression P would be above the maximum available boundary reaction; or when the reaction is mobilized only after some deformation occurs) where the pipeline is subjected to lower levels of both compression and elongation.

Similar effect is due to internal pressure increments. Although the Poisson effect would shorten the pipe when tensile hoop stresses are applied, the end cap effect (which is the axial tension due to the internal pressure acting in the internal cross section area) induces elongation. The net axial expansion

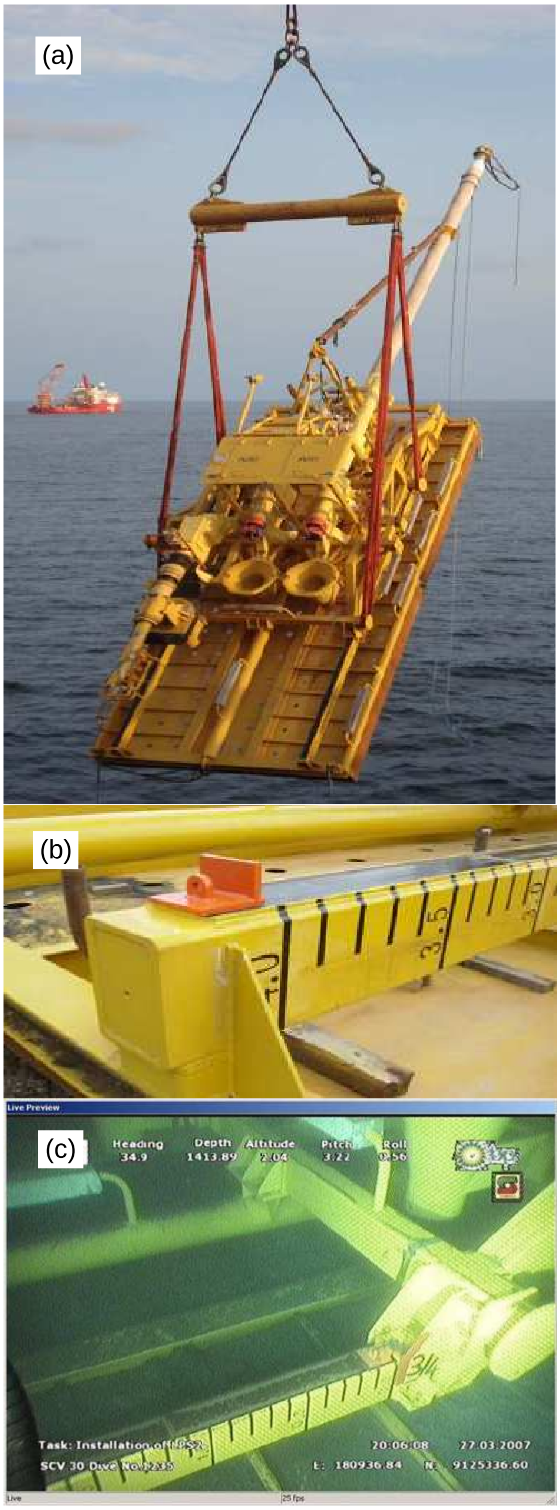

Figure 1 – PLET with sliding foundation – general view (a) and details (b and c) – reproduced from Jayson et al. (2008).

for a thin walled pipe results in a final length of $(1 + (\Delta p_i\ A_i(1\text{–}2\nu)/(E\ A_s)))L$ for a totally free pipeline; and the compression induced to a fully restrained pipeline is $P = \Delta p_i\ A_i(1\text{–}2\nu)$.

Since the axial expansion induced by the end cap effect is due to mechanical strain, in the fully restrained case the end cap force is directly transmitted to the boundary, and no compression is applied to the pipe steel wall. However, Palmer and Baldry (1974) showed that for global buckling assessment, the second order effect of the internal pressure is adequately accounted for if the end cap force is considered along with (i.e. added to) the compressive force acting in the pipe wall. The result of this summation is called “effective axial force”.

3.1 – Effective axial force

In a section of pipeline resting on the seabed, axial restraint is provided by the soil friction. The pipe-soil interaction is a complex non-linear phenomenon which has been extensively studied within the last decades, resulting in several publications (e.g. Cathie et al., 2005). The axial resistance is usually mobilized within small displacements, and after short length (in which the resistance varies non-linearly, in some cases presenting a peak followed by reduced values), the resistance vs. displacement curve stabilizes to a so called “residual” resistance. The magnitude of this final resistance per unit length of pipeline is typically very small if compared to the axial forces induced by HP/HT conditions, but after accumulating for a few kilometers of pipeline it might be enough to impose the fully restrained condition loads to its walls.

To illustrate, a 12.75in oil production flowline is studied as follows. The pipeline is approximately 4.5km long and will be subjected to the design loads shown in the temperature and pressure profiles depicted in Figure 2a. If the pipeline was fully restrained, the temperature and pressure would induce compressive axial force along the pipeline as described by the blue dashed line in Figure 2b. The temperature increment in this case is responsible for most of this load, being the corresponding parcel indicated by the green dotted line.

Actually, the axial compression builds up from zero at the pipeline's ends to a maximum value, approximately at its half length. The slope of the force diagram is the soil resistance per unit length. In Figure 2b, the maximum compressive force is far below that for the fully restrained condition.

The soil resistance per unit length could be higher as that of Figure 2c, in which the force diagrams would reach the blue dashed line and so (along the section where these lines are coincident) the compression is enough to induce the compressive mechanic strain to

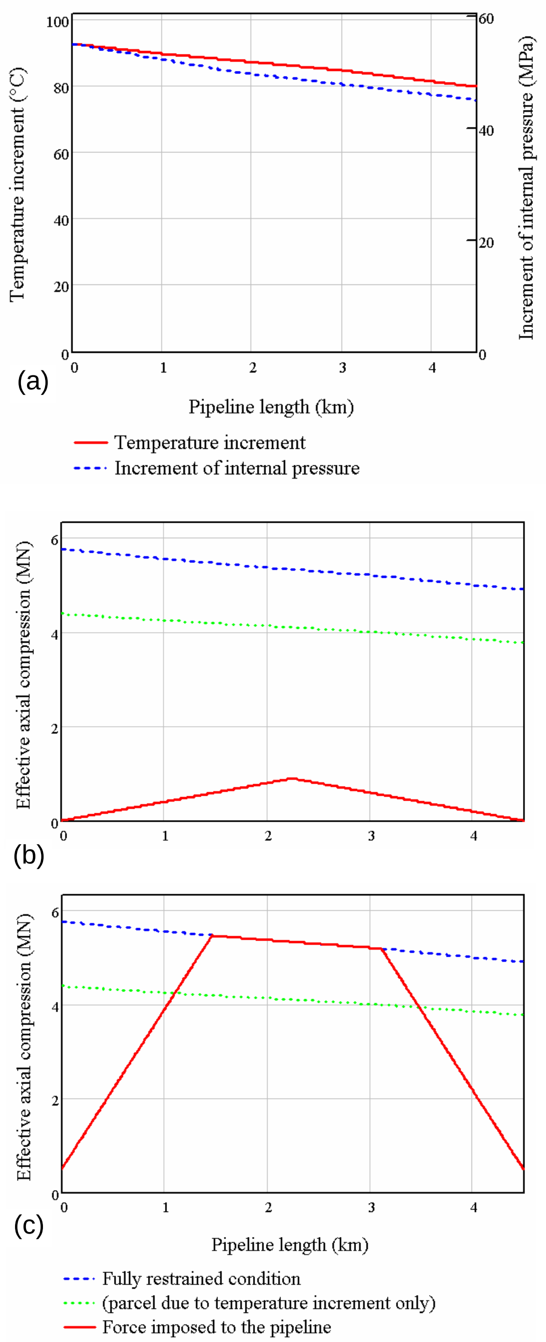

Figure 2 – 12.75in oil production pipeline – temperature and pressure profiles (a), axial compression diagrams (b and c) for different soil resistance conditions.

compensate the thermo-mechanical expansion due to both temperature and internal pressure. In addition, the force in Figure 2c builds up from a non-zero initial compression. This value corresponds to the axial soil resistance in PLETs. Other attachments installed along the pipeline would induce discontinuities to the axial force diagram (except if it is located in the fully restrained region).

3.2 – End expansion

Figure 3a present the axial displacement, compressive mechanic strain and thermo-mechanic expansion for the same conditions as in Figure 2c. The compressive mechanic strain is indicated as positive, so it has the same value of the thermo-mechanic expansion in the fully restrained region. It can be observed that the geometry of these two curves are alike the force diagrams.

As expected, the axial displacement in the fully restrained region is zero. For the left-hand side, the displacements are negative indicating that pipeline moves towards the left, up to a maximum (absolute) displacement of 0.95m at its left-hand side end. In opposition the rightmost region present positive displacements (towards the right). The end expansion at right-hand side is less than that for the other side as the load profiles (Figure 2a) decline along the pipeline length.

The expansion build up curve is approximately parabolic, as it is the integral of the net expansion (the difference between the compressive mechanic strain and thermo-mechanic expansion curves, corresponding to the hatched area).

The results in Figure 3b correspond to the conditions of Figure 2b. The large difference between the two curves result in an axial displacement diagram closer to a straight line. This curve does not present a fully restrained region with zero displacement and so, as the entire pipeline length is expanding, the end expansion results are higher than those in Figure 3a. It is observed, however, that the point for which the displacement is nil correspond with the maximum compressive strain (and thus with the maximum compressive force).

This observation is supported by the fact that the slope of the axial force diagram is the soil resistance per unit length. The nature of a frictional resistance is to act in the opposite direction of the movement. Hence, the reversion in slope (and thus in the direction of the soil resistance) correspond to the reversion in the direction of movement (from towards one side to towards the opposite), which shall occur (in a compatible displacement scheme) in the section where the displacement is zero.

When calculating the axial displacement by integrating the net expansion, one shall find the suitable integration constant to set the axial displacement zero at either the fully restrained region and/or at the soil resistance reversion points.

Pipelines such as that in Figure 3a are often called "long pipelines" while others as that in Figure 3b are called "short pipelines". The definition of "long" in this notation indicates only that the pipeline is long enough to the axial soil resistance build up to reach the fully restrained condition. It should be clear that it does not depend on the pipeline length only, but also on the loading and resistance. As abovementioned, both results in Figure 3 correspond to a same pipeline for different soil resistance conditions.

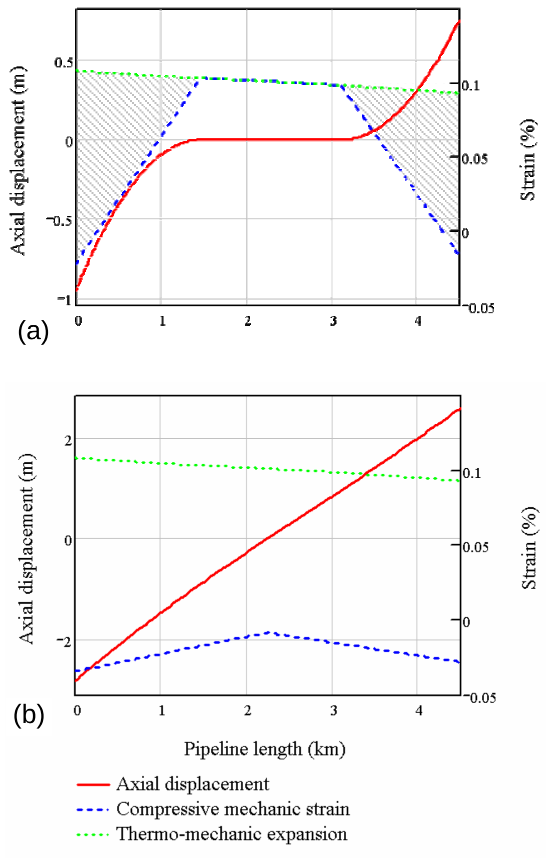

Figure 3 – Axial displacement, compressive mechanic strain and thermo-mechanic expansion for different soil resistance conditions (a and b).

3.3 – Lateral buckling

The curves shown in Figure 2 (b and c) and Figure 3 are result of analytical calculation from the pipeline length and cross-section properties, loading (Figure 2a) and nominal soil resistance values. The calculated compression, however, might induce the pipeline to buckle globally.

Pipeline global buckling is not necessarily a problem, as the stresses and strains in the bending might be within tolerable (safe) limits. Conversely, recent projects (e.g. Carneiro et al., 2009) have been using (and even forcing) controlled buckles to relief the axial compression.

When the pipeline buckles, its compression is reduced to a low level (which depends on the post buckle configuration and its global stiffness). The pipeline sections at the vicinity of the buckle will move towards the buckle, and the force diagram will have the corresponding slopes. Resulting force diagram can be built in the same graphical processes, by sketching the slopes from either the ends or the buckles to either adjacent slopes or the fully restrained condition envelope.

It should be observed that a pipeline that presents a fully restrained region in a first assessment, might not present it if buckles are accounted for. Several papers (e.g. Carr et al., 2003) discuss lateral buckling in deeper.

3.4 – Axial ratcheting

Results of finite element (FE) analyses of the same 12.75in 4.5km long pipeline are used to illustrate the axial ratcheting process. Together with the temperature and internal pressure increment profiles, analyses assume the bathymetry shown by the pipeline profile in Figure 4a, where the water depth is indicated along the pipeline length (using the “kilometer post” – KP – notation).

The analyses were performed using SAGE Profile 3D v2.0 (http://www.sage-profile.com). The program simulates the lay operation on the full three-dimensional seabed bathymetry; all the following phases of the pipeline life are then analyzed. The load history is maintained from the lay down, through water filled and hydro test conditions, up to the operational start-up/shutdown cycles.

The overall seabed slope observed in the bathymetry causes the pipeline weight to act not perpendicularly to the pipe axis, but with a small component (factored by the sine of the local slope angle) in its axial direction. This longitudinal component is resisted by the soil axial friction, interfering in the available net resistance that will build up the pipeline compression.

Figure 4b present the effective axial force diagram (compression is indicated here upwards but with negative signal). It is also sketched how the weight component is added to or subtracted from the nominal soil

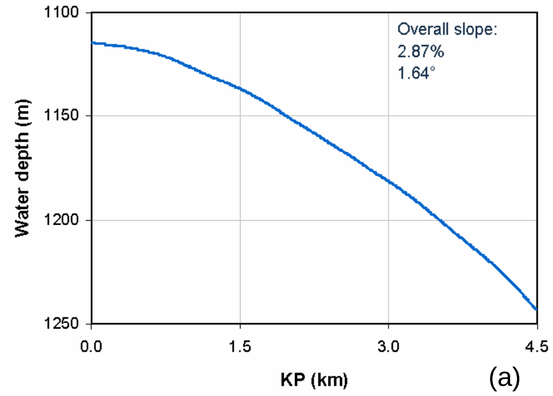

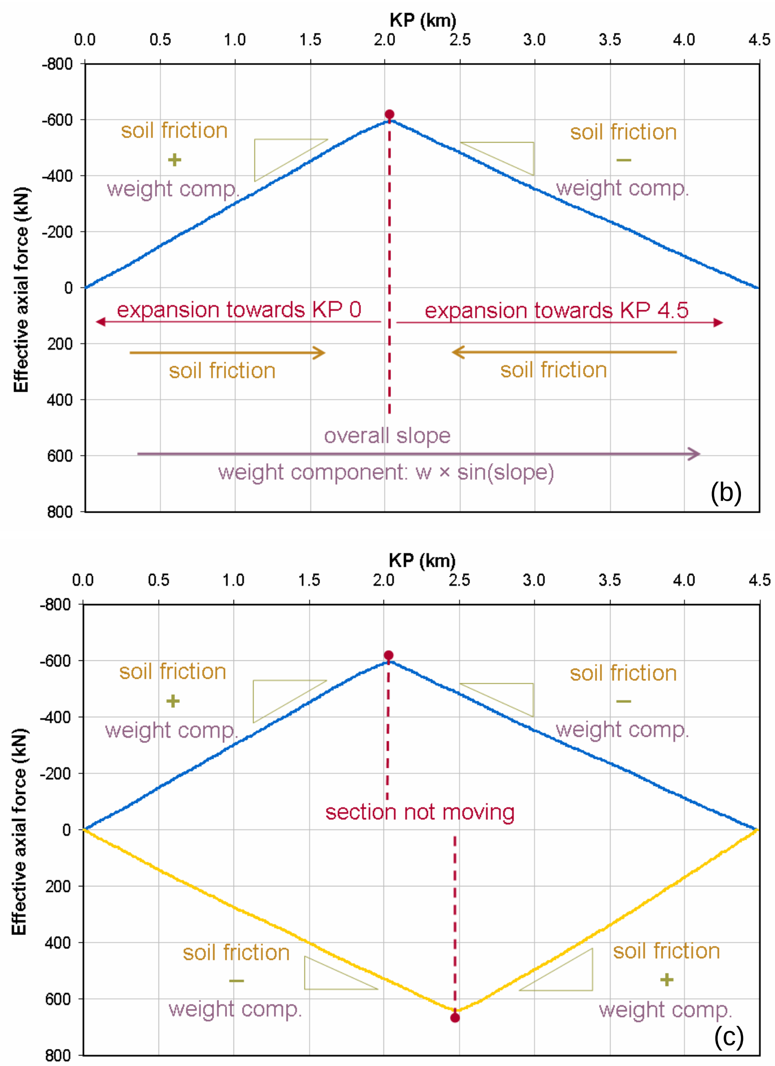

Figure 4 – Pipeline profile (a) and effective axial force diagrams (b and c).

resistance. As a result, the force diagram is not symmetrical, so the maximum point (which, as aforesaid, corresponds to the section not moving) is not at its half length.

If the pipeline is shut down so that its temperature and internal pressure are set back to their original (unloaded) values, the pipeline will tend to contract back to its original length. The soil friction will resist to this shortening also, so the pipeline will be under tension. In the same way, this tension will build up from zero at the ends up to a maximum value approximately at the pipelines half length.

As the weight component acts downwards always, the tension diagram at shut down will not be symmetric to the compression (loaded) curve, but as shown in Figure 4c. This asymmetry results in an offset (of some hundreds meters) between the section not moving during loading and unloading processes.

Figure 5a present the axial displacement diagram for first loading, showing the point not moving just after KP 2.0. When the pipeline is unloaded (Figure 5b), it contracts but not to its original position. The tension due to the soil resistance induces the residual expansion shown in yellow. As expected the point not moving (close to KP 2.5) continues in the same position as in the loaded condition, so the diagrams intersect. When loaded again (Figure 5c), the intersecting point is back about KP 2.0; and when shut down again, once more close to KP 2.5. The difference in these points induces the net axial shift indicated in Figure 5c. Both loaded and unloaded condition curves for the second cycle are similar to those for first cycle, but offset by this net axial shift of a few centimeters. Although small, this shift is accumulated at all further cycles (Figure 5d), hence for say some tens of cycles along the pipeline design life, is can accumulate into several meters of additional longitudinal displacement.

The presented results illustrate the axial ratcheting induced by an overall slope in the

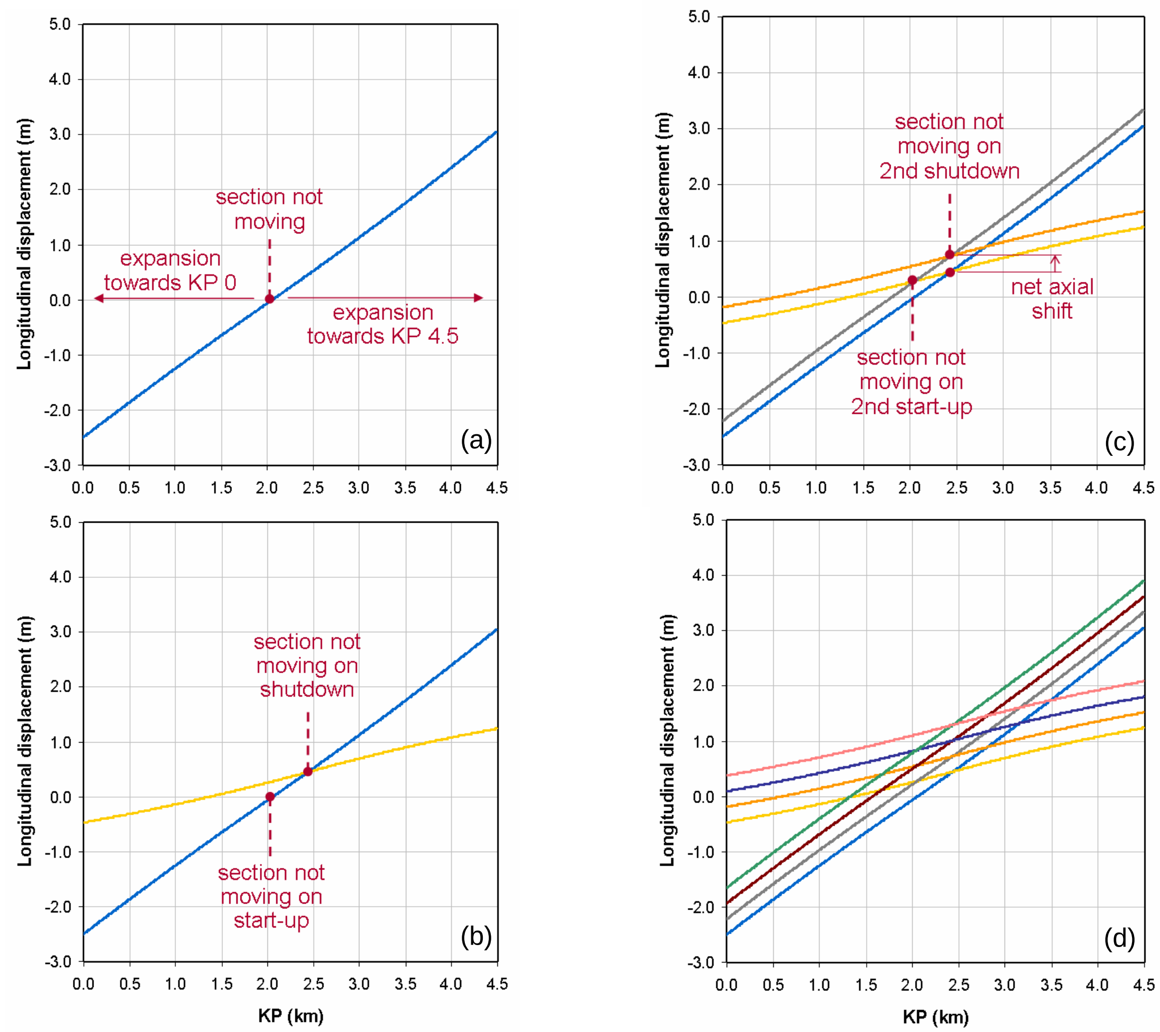

Figure 5 – Axial displacement diagrams for: (a) first loading; (b) first loading and first unloading; (c) firs and second cycle of loading and unloading; and (d) first four cycles of loading and unloading.

bathymetry, which is one of the pipeline walking mechanisms. Carr et al. (2006) describe this and other mechanisms, in which the walking is driven by either temperature transient or end tension (e.g. imposed by an in-line riser); a review of these mechanisms including a new driving effect is presented by Bruton et al. (2010).

4 – FE analysis of HP/HT pipelines with sliding PLETs

Finally, the design of a short HP/HT production rigid flowline with sliding PLETs is discussed over some FE analyses results. The pipeline under appraisal has the same cross sectional properties as the studied before but shorter length of 1.3km. As a result, the end expansion is not expressive, and a first assessment indicated that it could be fully within the range of reasonable sized sliding mechanisms in the PLETs' foundations. As long as this is true, the longitudinal force induced by the expansion to the PLETs (to be resisted by their foundations) is only the (usually negligible) friction in the mechanism.

The sliding mechanism was designed as sketched in Figure 6. The outward (extension) range of 1.5m would adequately cover the 0.65m maximum anticipated end expansion for first loading; and a 0.5m contingency inward range was also included. ROV operated locks keep the PLETs in the sketched configuration during installation. After released, the course is limited by end stoppers, which are not supposed to undergo loading in normal conditions.

Complete thermo-mechanical analyses were only performed after the PLETs were designed. Pipeline walking susceptibility was not identified in an early stage. First analyses considered no longitudinal end reaction, assumption in line with anticipated axial displacements within the sliding mechanism

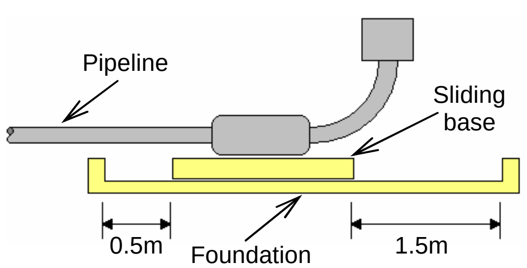

Figure 6 – Sketch of the PLETs' sliding mechanism.

range. The results however indicated walking downwards due to the seabed overall slope. After some load cycles, the accumulated displacement reached a point in which the upper end position during unloading (already considering the residual elongation) would go beyond inward (contingency) sliding range. The model with no longitudinal end reaction is then on unrealistic.

The thermo-mechanical analyses were performed again including non-linear boundary conditions at the ends to properly represent the full response of the designed sliding mechanisms. No reaction is imposed while the longitudinal displacement is within the designed range; further displacements are restrained.

The results in terms of effective axial force are presented in Figure 7. Up to the 18th loading, the diagrams coincide for all loading steps, as well as for all unloading steps. However, in the 18th unloading (shutdown), the sliding mechanism at the upper (left-hand side) end reaches the end of its course. An axial tensile force of 43kN is induced to this end in this step. In the next unloading step, the tensile PLET reaction is increased to 117kN, and then stabilizes in about 165kN for all further unloading steps.

The restraint provided by PLET at left-hand side end and the tendency to move towards the right results in a long pipeline section (approximately the leftmost 0.4km) with very small longitudinal displacement in the unloading condition. In this region, the soil axial resistance does not reach its residual value (as the resulting displacements are within the short mobilization length). The resistance (and thus the slope of the effective force diagram) varies along the length according to the displacement. As a result, the diagram is curved as observed in Figure 7.

Due to the unanticipated axial force induced to the PLETS, the sliding mechanism end stoppers had to be reassessed and strengthened as they would then have to withstand the calculated axial force in normal design condition. The PLETs' foundation was found incapable of safely undergoing such an horizontal load and mitigation measures had to be designed.

5 – Concluding remarks

Before dealing with the particular case of the PLETs with sliding foundation, the thermo-mechanical behavior of rigid flowlines under HP/HT conditions was reviewed. In special, the mechanics of longitudinal expansion; and ratcheting (pipeline walking) due to seabed slope were thoroughly assessed. Results of analytical calculations and FE analyses were used to illustrate the argumentation.

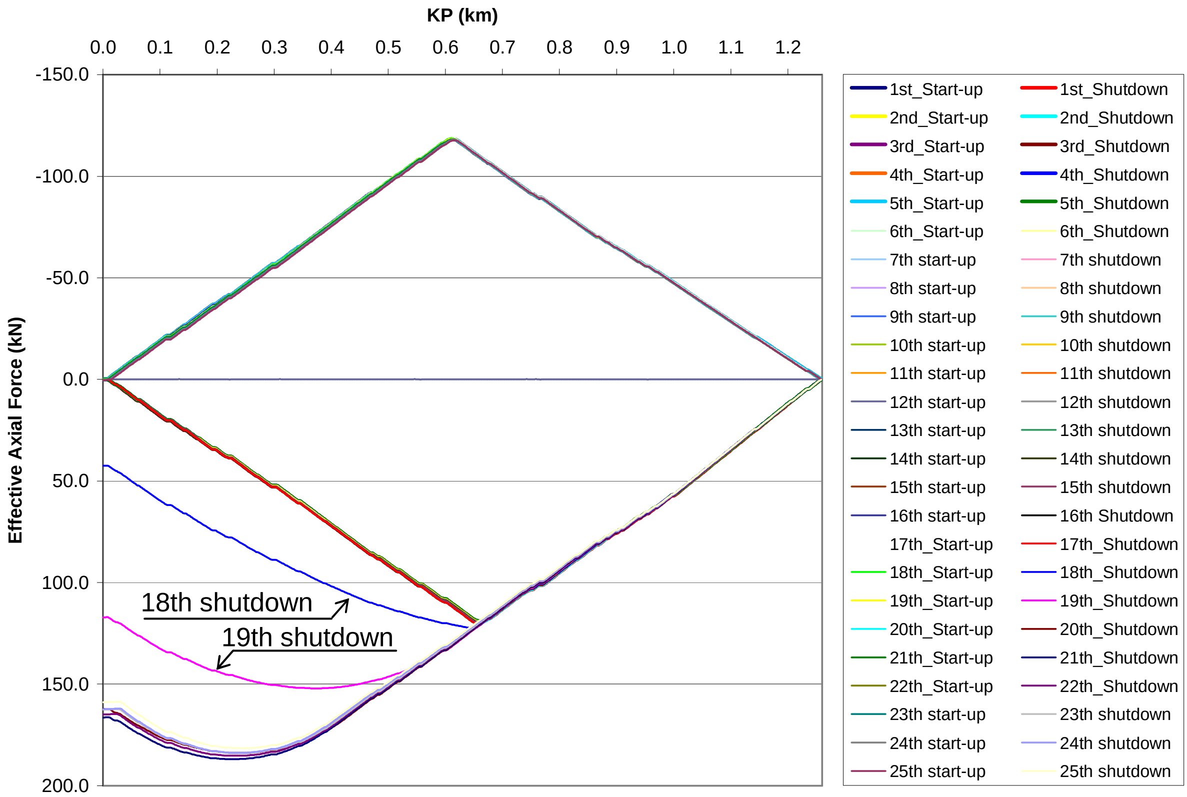

Figure 7 – Effective axial force diagram for pipeline with sliding PLETs – results for the first 25 cycles of loading and unloading.

The example of a short pipeline with sliding PLETs and high susceptibility of walking was then presented. Results show the necessity of using complex non-linear models with unusual boundary conditions to adequately anticipate the loading to the PLETs. It is also shown that the late identification of walking susceptibility might have major impact to the design.

6 – References

BRUTON, D. A. S., SINCLAIR, F., CARR, M. Lessons Learned From Observing Walking of Pipelines with Lateral Buckles, Including New Driving Mechanisms and Updated Analysis Models. In: Proceedings of the 42nd Offshore Technology Conference, Houston, USA, 2010.

CARNEIRO, D., GOUVEIA, J., PARRILHA, R., CARDOSO, C. O. Buckle Initiation and Walking Mitigation for HP/HT Pipelines. In: Proceedings of the Deep Offshore Technology Conference, Monte Carlo, Monaco, 2009.

CARR, M., BRUTON, D. A. S., LESLIE, D. Lateral Buckling and Pipeline Walking, a Challenge for Hot Pipelines. In: Proceedings of the 26th Offshore Pipeline Technology Conference, Amsterdam, the Netherlands, 2003.

CARR, M., BRUTON, D. A. S. Pipeline walking – understanding the field layout challenges, and analytical solutions developed for the Safebuck JIP. In: Proceedings of the 38th Offshore Technology Conference, Houston, USA, 2006.

CATHIE, D. N., JEACK, C., BALLARD, J. C., WINTGENS, J. -F. Pipeline Geotechnics – State-of-the-art. In: Gouvernec, Cassidy (eds), Frontiers in Offshore Geotechnics, Taylor & Francis Group, London, pp. 95-114, 2005.

JAYSON, D., DELAPORTE, P., ALBERT, J. -P., PREVOST, M. -E., BRUTON, D., SINCLAIR, F. Greater Plutonio project – Subsea Flowline Design and Performance. In: Proceedings of the 31st Offshore Pipeline Technology Conference, Amsterdam, the Netherlands, 2008.

PALMER, A. C., BALDRY, J. A. S. Lateral Buckling of Axially Constrained Pipelines. *Journal of Petroleum Technology*., v. 26, n. 11, pp. 1283-1284, 1974.